



OPEN Tb doped carbon dots as a platform for fluorescence ratiometric and colorimetric sensor for deferasirox

Fatemeh Latifi¹, Mohammad Amjadi¹, Tooba Hallaj²✉ & Seyyed Morteza Seyyed Alavi¹

Tb doped carbon dots (Tb-CDs) were synthesized by a simple hydrothermal method and the existence of Tb in the obtained CDs was confirmed by the several characterization methods. Tb-CDs were exploited to design a ratiometric fluorescence sensor for deferasirox (DFX) assay. CDs and Tb acted as reference and sensing prods in the sensor. In the presence of DFX, the fluorescence intensity of CDs remained unchanged, while Tb emission increased. The fluorescence ratio of Tb to CDs was proportional to the DFX concentration at the range of 0.1 to 2.5 μM . Additionally, the fluorescence color altered from blue (CDs emission) to green (Tb emission) with increasing DFX concentration. We employed this color variation to establish a smartphone based sensor for the DFX detection. The linear range of established sensor was 0.5–15 μM . The detection limit (3S) for the ratiometric and smartphone based sensor was calculated to be 0.08 and 0.4 μM , respectively. Both sensors were applied to measure DFX in human serum samples with satisfactory results.

Keywords Deferasirox, Lanthanide ions, Carbon dots, Ratiometric sensor, Smartphone

Carbon dots (CDs) are a class of carbon nanomaterials reported in 2004 for the first time¹. They are spherical nanoparticles with size less than 10 nm and amorphous carbon structure or in some cases, sp^2 -hybridized graphitic carbon. They exhibit unique physicochemical, optical, and electronic properties such as low toxicity, outstanding brightness, high solubility in water, thermal stability, chemical ineffective, and ease of use^{2,3}. Despite these unique properties, the limited number of functional groups in CDs (restricting the ability to interact with various compound) and low luminescence quantum yield can limit their applicability especially in the development of selective and sensitive luminescence sensors. Functionalizing the surface of CDs and doping them with heteroatoms have been found as suitable ways to improve the properties and extend the applicability of CDs. Chemical doping of CDs with heteroatoms and metal ions has attracted much attention due to economic and easy synthesis methods to amend their fluorescence properties^{4,5}. Various metal atoms such as Cu, Fe, Mn, Tb, Eu and so on have been doped into CDs for different purposes. The metal atoms doping procedure, resulting in the band structure modulation of CDs, can improve the optical properties and create novel functionalities for the doped CDs⁴.

Trivalent lanthanide ions (Ln^{3+}), especially Tb^{3+} and Eu^{3+} have attracted great attention as luminescence probes due to their unique spectroscopic properties, such as high Stokes shift, long luminescence lifetime, and narrow emission bands. These properties make them suitable choices for designing various fluorescence probes^{6,7}. However, Ln^{3+} suffer from low absorption coefficients and luminescence efficiency due to forbidden Laporte f-f transitions, restricting their application in luminescence probes. Various material and ligands have been applied to facilitate f-f transitions based on antenna effect. Ln^{3+} ions have a high affinity to oxygen-containing ligands or oxygen–nitrogen-containing organic compounds. When Ln^{3+} ions form complexes with suitable ligands that have strong absorption bands, the luminescence intensity of the system increases due to intramolecular energy transfer or antenna effect⁸. This phenomenon has been utilized for designing Ln^{3+} based fluorescence sensors to analyze various compounds including drugs that can act as a ligand^{9,10}.

On the other hand, concerning the exceptional optical properties of Eu^{3+} and Tb^{3+} , they have been applied as a dopant to design selective and sensitive CD based ratiometric fluorescence sensors^{11–13}. Compared to the traditional fluorescence sensors, more accurate and reliable results can be obtained by ratiometric sensors because of the elimination of environmental and instrumental noises. Additionally, the ratiometric fluorescence systems can be applied for establishing fluorescence color variation based sensors by smartphone or visual detection^{14,15}. Smartphone based sensors have been applied in various domains for on-site analysis, using their

¹Department of Analytical Chemistry, Faculty of Chemistry, University of Tabriz, Tabriz 5166616471, Iran. ²Cellular and Molecular Research Center, Cellular and Molecular Medicine Research Institute, Urmia University of Medical Sciences, Urmia, Iran. ✉email: Shhallaj@gmail.com

built-in cameras as a detector to measure the concentrations of different analytes¹⁶. For example, a ratiometric fluorescent sensor based on Eu-MOFs encapsulated CDs were applied for visual detection of Ag⁺ with naked eyes¹⁷. There are several reports about Tb and Eu doped CDs based ratiometric fluorescence sensors for visual detection of tetracyclines^{10,18,19}. Tb and Eu doped CDs were also used for the fluorescence ratiometric assay of dipicolinic acid^{20–23}.

Deferasirox (DFX) is the FDA approved tridentate iron chelator for the remedy of iron overload caused by blood transfusions, among individuals with thalassemia and myelodysplastic syndromes. The most common side effects of DFX include digestive disorders, skin rash, high serum creatinine, increased liver transaminases^{9,24}. It is important to monitor DFX concentration in biological fluid to evaluate its therapeutic effects and control its toxic effects. Various methods including chromatographic²⁵, electrochemical²⁶ and spectroscopic²⁷ methods have been reported for the determination of DFX. However, some of these methods experience shortages such as complicated and expensive equipment or unsuitable sensitivity and selectivity. Fluorescence sensors based on Tb⁹ and CDs^{28–30} have been individually applied for DFX sensing, but to the best of our knowledge there is no report about the application of Tb-doped CDs for the determination of DFX. Herein, Tb-doped CDs was used to design a ratiometric fluorescence sensor for DFX analysis. In this sensor, Tb acted as a sensing probe and CD acted as a reference. In the presence of DFX, as an organic ligand, the fluorescence intensity of Tb increased because of the energy transfer process from the ligand triplet state to Tb. The designed sensor was applied to measure DFX in human serum samples.

Experimental Apparatus

Tb-CDs shape and size distribution were studied using a transmission electron microscope (TEM; Philips EM 208, Germany). The functional groups of Tb-CDs were investigated using Fourier transform infrared (FT-IR) by Tensor 27 FT-IR spectrometer (Bruker, Germany). UV-Vis spectra were obtained using a spectrophotometer Carry 100 (Varian, Australia). Fluorescence spectra were recorded using a spectrofluorimeter FP-8300 (Jasco, Japan). X-ray diffraction pattern of Tb-CDs was obtained using a diffractometer Siemens D500 (Germany).

Reagent

All materials were of analytical grade. Deionized (DI) water were applied for all experiments. DFX, Tris-HCl buffer, Tb(NO₃)₃ and Folic acid were purchased from Sigma.

Synthesis of Tb-CDs

Tb-CDs were synthesized hydrothermally as the already reported process with a slight modification²¹. 0.03 g of folic acid and 0.078 g of Tb(NO₃)₃ were dissolved in DI water. After 20 min stirring, the pH of solution was adjusted at 4 by 1M NaOH and the final volume was reached to 30 ml. The solution was put inside the autoclave and heated in the oven at 180 °C for 6 h. For purification and removal of unreacted raw materials, the synthesized Tb-CDs were dialyzed against deionized water for three hours in a dialysis bag (2KD, Sigma).

Fluorescence ratiometric assay

For fluorescence analyses, 75 µl of Tb-CDs, 250 µl of Tris hydrochloride buffer (0.1 M, pH = 7.5), and different amounts of DFX or real samples were added to the test tube and reached 2 ml with DI water. Fluorescence spectra were recorded with the excitation wavelength of 270 nm and the fluorescence intensities were measured at the emission wavelengths of 440 and 546 nm.

Smartphone-based assay

Above-mentioned test solutions containing different amounts of DFX were transferred into a quartz cell and placed on the cell holder inside the box designed for the fluorescence color measurement under 254 nm UV light. A smartphone was placed on the top of the box (perpendicular to the light source) to monitor the color variation of solutions. RGB color intensities were obtained by the Camera RGB Color Picker program installed on the smartphone (Xiaomi Redmi Note 8, 48MP camera). The measurement was based on the changes in RGB color intensity of the prepared solutions.

Serum samples preparation method

Human plasma samples were obtained from Blood Transfusion Center (Tabriz, Iran). 2 ml of acetonitrile was added into a test tube containing 500 µl of serum sample for the precipitation of proteins. The mixture was centrifuged for 15 min at 6000 rpm. The supernatant was transferred into a 5-ml volumetric flask and adjusted to the final volume by DI water. At last, an appropriate volume of solution was put into the tube and measured according to the general procedure.

Results and discussion Characterization of Tb-CDs

Tb-CDs were prepared by a simple hydrothermal method from Tb(NO₃)₃ and folic acid as sources of Tb and C. TEM imaging (Fig. 1a) indicated the nanoparticles with sizes smaller than 10 nm²¹. In the presence of Tb(NO₃)₃, the polymerization of folate molecules was restricted because of the electrostatic repulsion caused by Tb³⁺ ions. It leads to the formation of relatively small Tb-CD particles.

The structural features of Tb-CDs including the surface moieties and existing elements was studied by FT-IR and EDS analyses. For comparison, undoped CDs were also synthesized by the same method using only folic acid. FT-IR spectra confirm the existence of C=C, C=O, C-N, NH₂, NH and OH on the surface of both

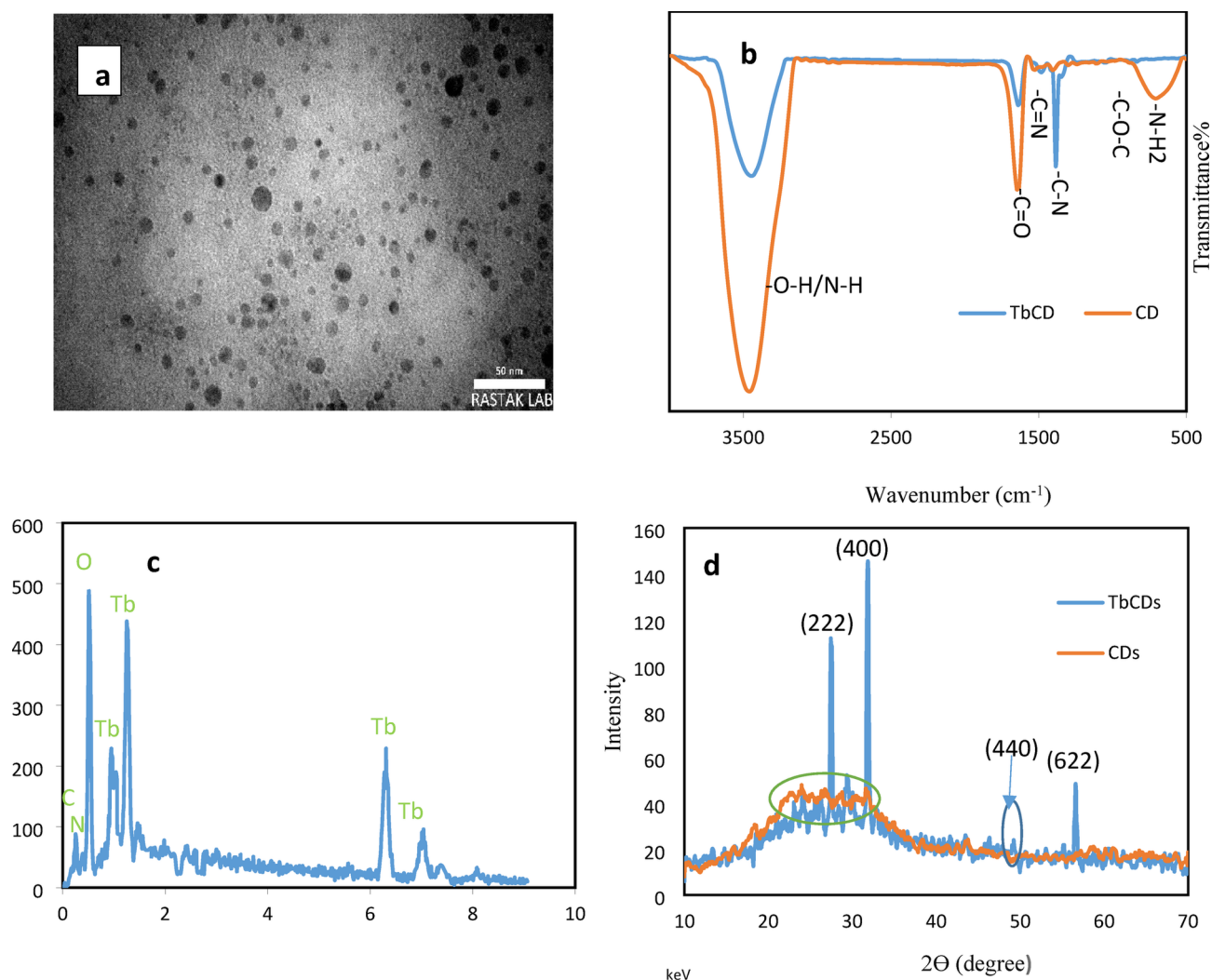


Fig. 1. (a) TEM image, (b) FT-IR spectra, (c) EDS spectrum, and (d) XRD pattern of CDs and Tb-CDs.

CDs. As can be seen in Fig. 1b, the appeared peaks in FT-IR spectra of CDs and Tb-CDs are almost the same. However, the intensity of some peaks such as C=O, C-N and NH₂ decreased in Tb-CDs which can be related to the complex formation between Tb and these functional groups²¹. Furthermore, EDS results indicate that CDs contain 26.24, 37.21, 36.55 W% of N, C, O elements (ESI, Fig. S1), and Tb-CDs include 28.64, 17.45, 15.91, 37.99 W% of N, C, O, Tb elements (Fig. 1c).

X-ray diffraction (XRD) pattern (Fig. 1d) was used to ensure the synthesis of Tb-CDs. A peak appeared around $2\theta = 25$ is related to the amorphous structure of CDs³¹. The characteristic peaks of Tb were appeared in 27.6° (222), 32° (400), 49° (440), 56.66° (622), confirming existence of Tb in the structure of Tb-CDs^{32,33}.

The optical features of Tb-CDs and CDs were studied by recording fluorescence and UV-vis absorption spectra (Fig. 2a). The fluorescence spectra of both CDs were independent of the excitation wavelength, and the highest emission intensity for CDs (Fig. S1) and Tb-CDs (Fig. 2b) was observed at the 360 and 270 nm excitation wavelength, respectively. The emission peaks appeared at 490, 546, 590 and 625 nm are related to Tb. The appearance of these peaks indicated the successful synthesis of Tb-CDs. The quantum yield % (QD%) of Tb-CDs was calculated to be 73.5%. Two obvious absorption peaks at 235 and 284 nm and a shoulder at 339 nm were appeared at the UV-Vis spectra of CDs. The mentioned peaks can be assigned to the $\pi-\pi^*$ transition of the aromatic carbon ring, $\pi-\pi^*$ transition of C=C bond and $n-\pi^*$ transition of the C=O or C=N bond, respectively^{34,35}. In the absorption spectrum of Tb-CDs (Fig. 2a) there is apparently a blue-shift for the peak around 235 nm and it is no longer a distinct peak compared to CDs²¹. Above-mentioned characterizations were confirmed that Tb was successfully doped in the structure of CDs.

Fluorescence sensor based on Tb-CDs for DFX assay

We exploited the prepared Tb-CDs to develop a fluorescence ratiometric sensor for the determination of DFX. In the absence of DFX (Fig. S2a), the fluorescence intensity of Tb at 546 nm is too low due to the low absorption factor of Tb³⁺, stemming from Laporte forbidden f-f transitions. After addition of DFX, no significant change in the fluorescence intensity of Tb-CDs at 440 nm was observed, but Tb³⁺ fluorescence peaks at 546, 590, 625

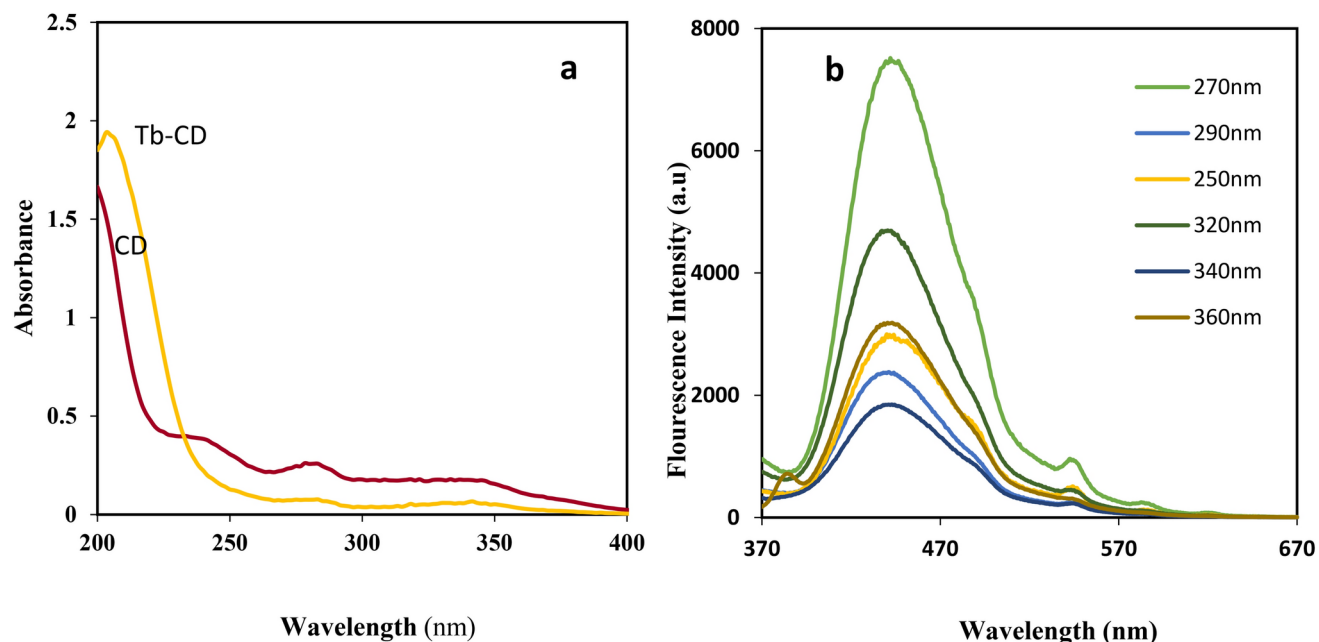


Fig. 2. (a) UV-vis absorption spectra of CDs and Tb-CDs, (b) Fluorescence spectrum of Tb-CD.

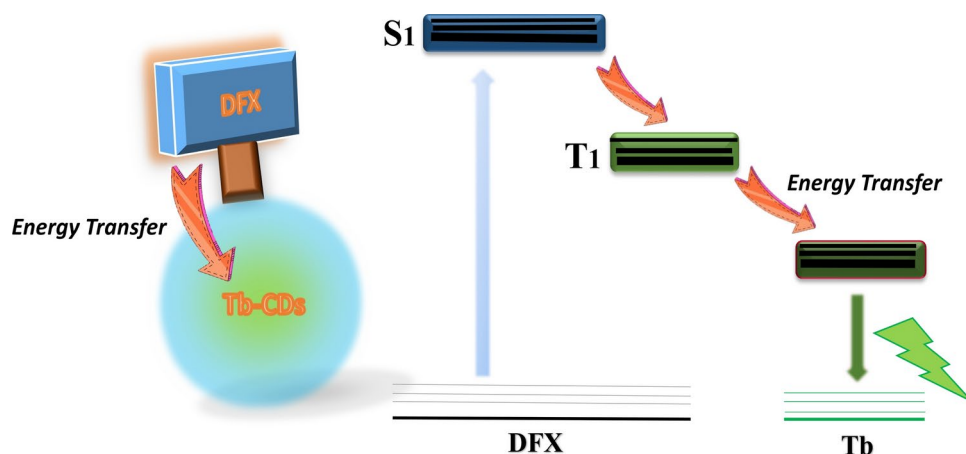


Fig. 3. The sensing mechanism of DFX by Tb-CDs based on antenna effect.

nm were significantly intensified (Fig. S2b). It can be attributed to the antenna effect of DFX which acts as an organic ligand and forms a complex with Tb^{3+} . The antenna effect is an intramolecular energy transfer between oxygen–nitrogen-containing organic compounds such as DFX and terbium ions. In fact, the photons were absorbed by DFX and then the energy transfer process occurs from the triplet state of the ligand (DFX) to the terbium ion and its fluorescence signal increases (Fig. 3). This phenomenon inspires us to design the DFX ratiometric fluorescence sensor using CDs and Tb peaks as a reference and sensing probe, respectively. Additionally, concerning the different emission color of Tb (green) and CDs (blue), we developed a fluorescence colorimetric method to measure the DFX by a smartphone.

It is worth mentioning that the mixture of CDs and Tb with the same concentrations, applying in the synthesis of Tb-CDs, was prepared and utilized for DFX measurement. As shown in Fig S3, the fluorescence intensity variations of Tb in the presence of various concentration of DFX are too low, indicating low sensitivity of the mixture of Tb and CDs for DFX measurement compared to the synthesized Tb-CDs. The results confirmed the necessity of hydrothermal synthesis of Tb-CDs to achieve more sensitive sensor for DFX detection.

Analytical performance of fluorescence sensor

To obtain maximum sensitivity for DFX sensing, the influence of factors such as amount of Tb-CDs, pH, kind and concentration of buffer, incubation time and temperature on the fluorescence signal were examined (Fig. S4). DFX measurements were done under obtained optimum condition (including 75 μL of Tb-CDs, Tris–

HCl buffer, 0.0125 M, pH=7.5, at room temperature with 5 min incubation time.) As shown in Fig. 4, with increasing the concentration of DFX, the emission intensity at the 440 nm peak remains constant while the emission intensity at the 546 nm peak increases. We applied the fluorescence intensity ratio (F_{546}/F_{440}) as an analytical signal for DFX measurement. A linear relationship was obtained in the range of 0.1–2.5 μM with the detection limit 0.08 μM ($S/N = 3$) for the determination of DFX. The method's reproducibility was examined by the calculation of relative standard deviation (RSD) for five replicate analyses of 0.2 μM , which were 1.2%.

On the other hand, with the increase of DFX concentration, the intensity of Tb^{3+} green emission (at 546 nm) increased, while the intensity of blue emission (at 440 nm) of CDs was constant. As a result, the color of solutions under UV radiation varied from blue to green. We followed up RGB signal (the intensity of red, green and blue color recorded by the smartphone) as an analytical response. As shown in Fig. 5, there was a linear relationship between B component (the intensity of blue color) and the concentration of DFX in the range of 0.5–15 μM . In this way, we designed a smartphone-based fluorescence colorimetric sensor using Tb-CDs to measure DFX. The detection limit and RSD% (for 1.5 μM) of developed sensor were calculated to be 0.4 μM and 3.8%, respectively.

We evaluated the selectivity of both sensors by investigating the effect of some species found in biological samples on the measurement of DFX (1.0 μM). The concentration ratio of interferences was calculated with a relative error of <5%. The results reported in (Table 1) and (Table S1) indicated the appropriate selectivity of developed methods.

Compared to already reported fluorescence methods (Table 2)^{28–30,36}, the established ratiometric method indicated better analytical performance, as well as making it possible to simply measure DFX by the smartphone instead of the spectrofluorimeter. Compared to the Tb sensitized fluorescence method⁹ for the DFX determination (our group's previous work), the selectivity of this sensor specially in the presence of transition metal ions including Fe, Zn and Cu was improved and consumption of materials (especially expensive Tb salt) was reduced. Against some reported methods which suffer from complicated synthesis of fluorescence probe³⁶ or need to use a quencher to DFX assay^{28–30}, the applied fluorescence probe was synthesized by a simple method and no need to use other elements for designing the sensor.

Real sample analysis

We investigated the applicability of established sensors for the determination of DFX in human serum samples. DFX measurement in human serum samples was done by both spectrofluorimeter and smartphone. The samples were spiked with DFX in the therapeutic concentration range^{37,38}. The recoveries were obtained in the range of 97–105%. Moreover, the Student's t-test values were calculated for all analyses and indicated the accuracy of developed methods. The results are reported in Tables 3 and 4.

Conclusion

In this study, we used the one-step hydrothermal method for the synthesis of Tb-CDs and characterized them by spectroscopic and microscopic methods. Tb-CDs were used to develop a ratiometric fluorescence method for the measurement of DFX. With increasing DFX concentration, the Tb fluorescence peak increased while the peak corresponding to the CDs remained constant. The improvement of Tb fluorescence intensity was assigned to the antenna effect of DFX, leading to the energy transfer process from DFX to the terbium ion. The increase of Tb to CDs fluorescence signal ratio was proportional to the DFX concentration. Beside, considering the color variation of emitted light from blue to green, related to the change in the ratio of the two fluorescence peaks

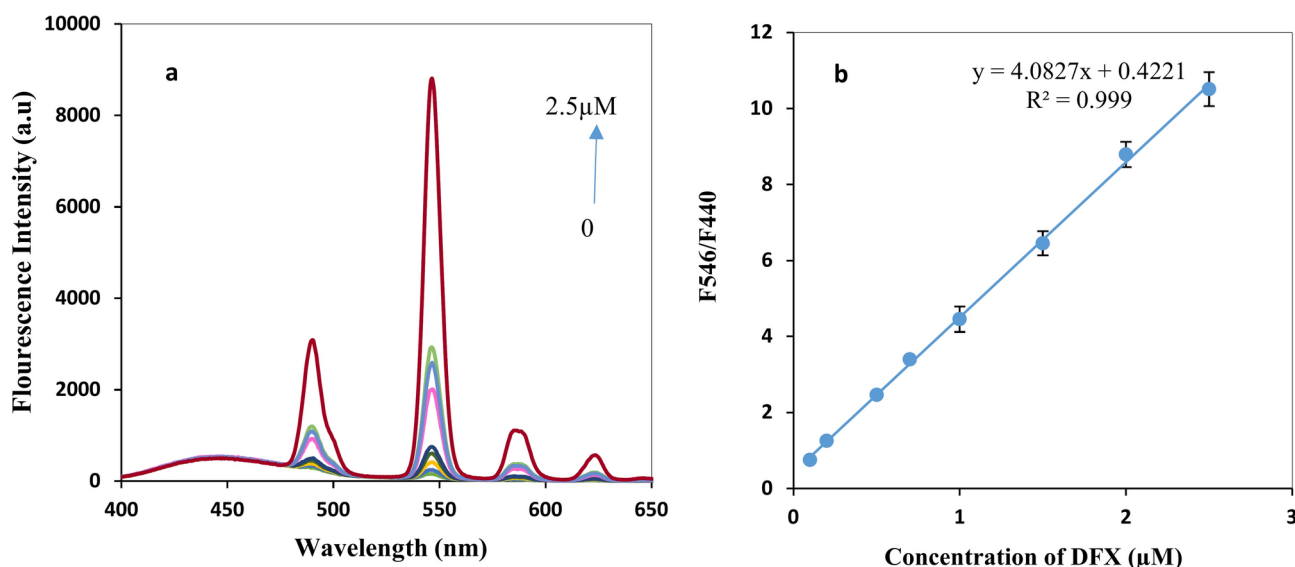
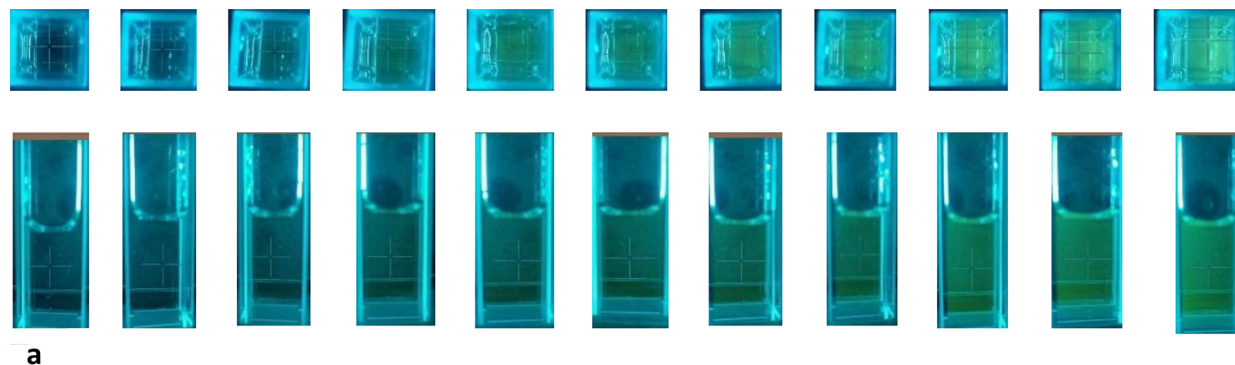


Fig. 4. (a) Fluorescence spectrum of Tb-CD in the presence of DFX different concentrations (0.1–2.5 μM), and (b) corresponding ratiometric calibration curve under optimal conditions.



a

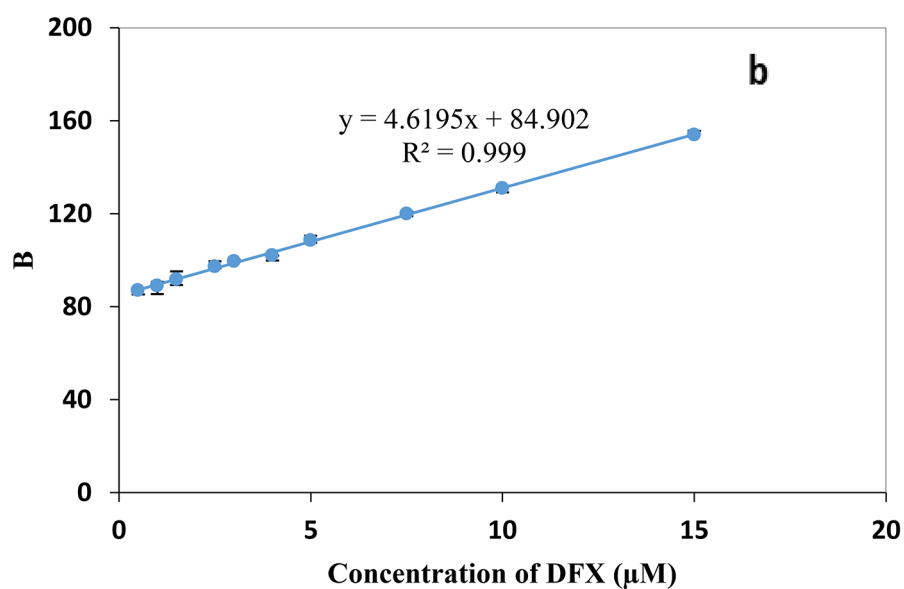


Fig. 5. (a) Emission color change of Tb-CDs in the presence of DFX different concentrations (0–15 μM) under 254 nm UV light. (b) Calibration curve for detection of DFX by smartphones.

Coexisting substance	Tolerance limit
Na ⁺ , K ⁺ , Cl [−] , Sucrose, Lactose, L-cysteine, Glucose, Alanine, Ca ²⁺ , SO ₄ ^{2−}	1000
Mg ²⁺ , NO ₃ [−] , I [−]	800
Deferiprone	600
Glutathione	500
Ascorbic acid, F [−] , Uric acid	400
Creatinine, Urea	200
Glycine, Lactic Acid, Tryptophan	100
Fe ³⁺ , Cu ²⁺ , Zn ²⁺	50

Table 1. Tolerance limits of some potentially interfering species in the determination of 1 μM DFX.

(546 and 440), a smartphone-based colorimetric method was designed for measuring DFX. Both sensors were successfully used to measure DFX in biological samples.

Fluorescence sensor	Detection method	Linear range (μM)	Limit of detection (μM)	Reference
CDs-Cu	Quenching	1.33–53.5	0.88	29
Tb ³⁺	Terbium-sensitized fluorescence	0.005–5	0.0015	9
CDs-Cu	Quenching	1.33–53.5	0.32	28
MPT ^a	Quenching	20–100	–	36
DA-CDs-Cu	Quenching and recovery	2.67–26.7	1.60	30
Tb-CDs	Ratiometric	0.1–2.5	0.08	This work
Tb-CDs	Fluorescence colorimetry	0.5–15	0.4	This work

Table 2. Comparison between analytical performance of developed methods and some reported fluorescence methods for the determination of DXF. ^aA thiourea-based diphenyl acetamide probe.

Sample	Added (μM)	Founded (μM) ^a	Recovery \pm RSD%	t-Statistic ^b
Serum 1	0	0.0	–	–
	50	49.70 \pm 1.4	99.4 \pm 2.9	0.3
	100	99.8 \pm 4.8	99.8 \pm 4.8	0.05
Serum 2	0	0.0	–	–
	50	49.0 \pm 3.5	98.0 \pm 7.2	0.4
	100	104.5 \pm 7.8	104.5 \pm 7.5	0.9

Table 3. DXF determination in serum samples by ratiometric fluorescence method. ^aMean of three determinations \pm standard deviation. ^bt-critical = 4.3 for n = 2, p = 0.05.

Sample	Added (μM)	Founded (μM) ^a	Recovery \pm RSD%	t-Statistic ^b
Serum 1	0	0.0	–	–
	50	49.2 \pm 2.2	98.4 \pm 4.6	0.6
	100	97.6 \pm 3.2	97.6 \pm 3.1	0.6
Serum 2	0	0.0	–	–
	50	51.0 \pm 1.8	102.0 \pm 3.5	0.9
	100	95.7 \pm 2.5	95.7 \pm 2.6	1.9

Table 4. DXF determination in serum samples by smartphone-based method. ^aMean of three determinations \pm standard deviation. ^bt-critical = 4.3 for n = 2, p = 0.05.

Data availability

The data and materials are available from the corresponding author on reasonable request.

Received: 5 March 2025; Accepted: 2 April 2025

Published online: 24 May 2025

References

- Xiao, P. et al. Photoluminescence immunoassay based on grapefruit peel-extracted carbon quantum dots encapsulated into silica nanospheres for p53 protein. *Biochem. Eng. J.* **139**, 109–116 (2018).
- Zheng, X. T., Ananthanarayanan, A., Luo, K. Q. & Chen, P. Glowing graphene quantum dots and carbon dots: Properties, syntheses, and biological applications. *Small* **11**, 1620–1636 (2015).
- Shinde, R. et al. Argyreia nervosa-derived carbon dots for highly sensitive and selective epinephrine detection. *Inorg. Chem. Commun.* **174**, 113976 (2025).
- Ansari, L., Hallaj, S., Hallaj, T. & Amjadi, M. Doped-carbon dots: Recent advances in their biosensing, bioimaging and therapy applications. *Colloids Surf. B* **203**, 111743 (2021).
- Tejwan, N. et al. Metal-doped and hybrid carbon dots: A comprehensive review on their synthesis and biomedical applications. *J. Control. Release* **330**, 132–150 (2021).
- Cui, Y., Chen, B. & Qian, G. Lanthanide metal-organic frameworks for luminescent sensing and light-emitting applications. *Coord. Chem. Rev.* **273–274**, 76–86 (2014).
- Hallaj, T. et al. Terbium-to-quantum dot Förster resonance energy transfer for homogeneous and sensitive detection of histone methyltransferase activity. *Nanoscale* **12**, 13719–13730 (2020).
- Dossantos, C., Harte, A., Quinn, S. & Gunnlaugsson, T. Recent developments in the field of supramolecular lanthanide luminescent sensors and self-assemblies. *Coord. Chem. Rev.* **252**, 2512–2527 (2008).
- Manzoori, J. L. et al. Terbium-sensitized fluorescence method for the determination of deferasirox in biological fluids and tablet formulation. *Luminescence* **26**, 244–250 (2011).
- Fan, Y. J. et al. A dual-signal fluorescent colorimetric tetracyclines sensor based on multicolor carbon dots as probes and smartphone-assisted visual assay. *Anal. Chim. Acta* **1247**, 340843 (2023).

11. Han, Y. et al. Impact on ratiometric fluorescence of carbon dots hybridizing with lanthanide in determination of residual Carbendazim in food. *Appl. Surf. Sci.* **606**, 154700 (2022).
12. Bao, J. et al. A ratiometric lanthanide-free fluorescent probe based on two-dimensional metal-organic frameworks and carbon dots for the determination of anthrax biomarker. *Microchim. Acta* **188**, 84 (2021).
13. Zhong, Q., Chen, T., Zhang, M. & Chen, X. Ratiometric fluorescence sensing of triclosan by lanthanide-functionalized metal-organic frameworks. *Microchem. J.* **206**, 111598 (2024).
14. Liu, L., Ga, L. & Ai, J. Ratiometric fluorescence sensing with logical operation: Theory, design and applications. *Biosens. Bioelectron.* **213**, 114456 (2022).
15. Kayani, K. F. et al. Ratiometric fluorescence detection of tetracycline in milk and tap water with smartphone assistance for visual pH sensing using innovative dual-emissive phosphorus-doped carbon dots. *Food Control* **164**, 110611 (2024).
16. Kayani, K. F. & Abdullah, A. M. Eco-friendly fluorescent detection method for Cu²⁺ ions combined with smartphone-integrated paper strip sensors based on highly fluorescent 2-aminoterephthalic acid in milk samples. *J. Food Compos. Anal.* **135**, 106577 (2024).
17. Zhang, Y. et al. Strongly emissive formamide-derived N-doped carbon dots embedded Eu(III)-based metal-organic frameworks as a ratiometric fluorescent probe for ultrasensitive and visual quantitative detection of Ag⁺. *Sens. Actuators B Chem.* **339**, 129922 (2021).
18. Jia, L. et al. A stick-like intelligent multicolor nano-sensor for the detection of tetracycline: The integration of nano-clay and carbon dots. *J. Hazard. Mater.* **413**, 125296 (2021).
19. Sang, Y. et al. Color-multiplexing europium doped carbon dots for highly selective and dosage-sensitive cascade visualization of tetracycline and Al³⁺. *Sens. Actuators B Chem.* **362**, 131780 (2022).
20. Zhou, Q. et al. A design strategy of dual-ratiometric optical probe based on europium-doped carbon dots for colorimetric and fluorescent visual detection of anthrax biomarker. *Talanta* **222**, 121548 (2021).
21. Tian, X. & Fan, Z. Comparison between terbium-doped carbon dots and terbium-functionalized carbon dots: Characterization, optical properties, and applications in anthrax biomarker detection. *J. Lumin.* **244**, 118732 (2022).
22. Liu, M. L. et al. Anthrax biomarker: An ultrasensitive fluorescent ratiometry of dipicolinic acid by using terbium(III)-modified carbon dots. *Talanta* **191**, 443–448 (2019).
23. Zhang, L. et al. Terbium functionalized schizochytrium-derived carbon dots for ratiometric fluorescence determination of the anthrax biomarker. *Nanomaterials* **9**, 1234 (2019).
24. Katzung, B. G. (ed.) *Basic & Clinical Pharmacology* Fourteenth. (McGraw-Hill, 2018).
25. Li, T. et al. A simple LC–MS/MS method for determination of deferasirox in human plasma: Troubleshooting of interference from ferric ion in method development and its application. *J. Pharm. Biomed. Anal.* **151**, 145–150 (2018).
26. Baker, F. H. M., Saleh Mashkour, M. & Adnan AL-Khafagi, H. Electrochemical determination of anti-thalassemia drug (deferasirox) by cyclic voltammetry technique using GCE modified with MWCNTs electrode. *Mater. Today Proc.* **61**, 758–765 (2022).
27. Li, N. et al. Cu²⁺-mediated telomeric dimeric G-quadruplex DNAzyme for highly sensitive colorimetric detection of deferasirox. *Talanta* **283**, 127116 (2025).
28. Wang, Y. et al. Effective synthesis of fluorescent carbon dots and their application in controllable detection of deferasirox. *Microchem. J.* **206**, 111536 (2024).
29. Han, W. et al. A signal-off fluorescent strategy for deferasirox effective detection using carbon dots as probe and Cu²⁺ as medium. *Anal. Chim. Acta* **1179**, 338853 (2021).
30. Wang, C.-C., Huang, P.-T., Shang Kou, H. & Wu, S.-M. Cu²⁺-induced quenching and recovery of the luminescence of dopamine-conjugated carbon dots for sensing deferasirox in plasma. *Sens. Actuators B Chem.* **311**, 127916 (2020).
31. Li, J. et al. Folic acid-modified cerium-doped carbon dots as photoluminescence sensors for cancer cells identification and Fe(III) detection. *Chemosensors* **10**, 219 (2022).
32. Tang, Q. et al. Preparation, characterization and optical properties of terbium oxide nanotubes. *J. Mater. Chem.* **13**, 3103 (2003).
33. Belaya, S. V. et al. Terbium oxide films grown by chemical vapor deposition from terbium(III) dipivaloylmethanate. *Inorg. Mater.* **50**, 379–386 (2014).
34. Jiang, K. et al. Triple-mode emission of carbon dots: Applications for advanced anti-counterfeiting. *Angew. Chem. Int. Ed.* **55**, 7231–7235 (2016).
35. Zhang, R. & Chen, W. Nitrogen-doped carbon quantum dots: Facile synthesis and application as a “turn-off” fluorescent probe for detection of Hg²⁺ ions. *Biosens. Bioelectron.* **55**, 83–90 (2014).
36. Khurshid, K. et al. Highly sensitive AIEE active fluorescent probe for detection of deferasirox: extensive experimental and theoretical studies. *RSC Adv.* **14**, 21682–21691 (2024).
37. Piolatto, A. et al. Pharmacological and clinical evaluation of deferasirox formulations for treatment tailoring. *Sci. Rep.* **11**, 12581 (2021).
38. Galanello, R., Campus, S. & Origa, R. Deferasirox: Pharmacokinetics and clinical experience. *Expert Opin. Drug Metab. Toxicol.* **8**, 123–134 (2012).

Acknowledgements

The authors acknowledge Urmia University of Medical Sciences for the support provided (Project number: 13402, approved by the Research Ethic Committee at the Urmia University of Medical Sciences, Ethical code: IR.UMSU.REC.1403.266).

Author contributions

Fatemeh Latifi: Investigation, Validation, Formal analysis, Writing—Original Draft. Mohammad Amjadi: Supervision, Resources, Methodology, Validation, Writing—review & editing. Tooba Hallaj: Conceptualization, Resources, Methodology, Formal analysis, Writing—Review & Editing. Seyyed Morteza Seyyed Alavi: Validation.

Funding

The authors acknowledge Urmia University of Medical Sciences for the support provided (Project number: 13402).

Declarations

Competing interests

The authors declare no competing interests.

Ethical approval

This study was approved by the Research Ethic Committee at the Urmia University of Medical Sciences, Ethical code: IR.UMSU.REC.1403.266.

Additional information

Supplementary Information The online version contains supplementary material available at <https://doi.org/10.1038/s41598-025-97035-x>.

Correspondence and requests for materials should be addressed to T.H.

Reprints and permissions information is available at www.nature.com/reprints.

Publisher's note Springer Nature remains neutral with regard to jurisdictional claims in published maps and institutional affiliations.

Open Access This article is licensed under a Creative Commons Attribution-NonCommercial-NoDerivatives 4.0 International License, which permits any non-commercial use, sharing, distribution and reproduction in any medium or format, as long as you give appropriate credit to the original author(s) and the source, provide a link to the Creative Commons licence, and indicate if you modified the licensed material. You do not have permission under this licence to share adapted material derived from this article or parts of it. The images or other third party material in this article are included in the article's Creative Commons licence, unless indicated otherwise in a credit line to the material. If material is not included in the article's Creative Commons licence and your intended use is not permitted by statutory regulation or exceeds the permitted use, you will need to obtain permission directly from the copyright holder. To view a copy of this licence, visit <http://creativecommons.org/licenses/by-nc-nd/4.0/>.

© The Author(s) 2025